Frequency-Domain Homogenization of Bundles of Wires in 2D Magnetodynamic FE Calculations

Johan Gyselinck and Patrick Dular

Abstract— **A general approach for the frequency-domain homogenization of multi-turn windings in 2D FE calculations is presented. First a skin and proximity effect characterization of the individual conductors, of arbitrary cross-section and packing, is obtained using a representative 2D FE model. Herein three excitation modes are considered, viz current and flux density in two perpendicular directions. In practical cases, the three modes are independent and the obtained frequency-dependent impedance and complex reluctivity tensor can be readily used in a FE model of the complete device. By way of example and validation, the method is applied to an inductor having an airgap and one of three different windings. The homogenized model produces global results (impedance versus frequency) that agree well with those obtained with a more precise FE model. In the latter each turn of the winding is explicitly modelled and finely discretized.**

Keywords— **Skin effect, proximity effect, eddy currents, finite element methods.**

I. Introduction

Multiturn windings in electromagnetic devices operated at sufficiently high frequency may display considerable eddy current losses. This constitues a major design aspect for, e.g., swiched mode power supply (SMPS) transformers. Unfortunately, the analytical approaches proposed in literature over the last decades do not garantee satisfactory results for all practical applications [1], [2], [3], [4], [5]. They may therefore be advantageously combined with numerical methods, in particular the finite element (FE) method [6], [7].

The brute-force FE approach, which consists in explicitly modelling and finely discretizing each separate turn of a winding in a (2D of 3D) FE model, remains to date too computationally expensive for it to be a practical design tool. The use of homogenization methods is imperative, see, e.g., [8] for a general and mathematical approach. Their application to windings is not yet common practice. In the frequency domain, proximity effect and associated losses can be effected by adopting a complex permeability (or reluctivity), the (frequency-dependent) expression of which is either obtained analytically [4] or using an elementary FE model [7], [9]. The latter method has been mainly used for a rectangular packing of round conductors.

In this paper we propose a generalization of this approach, allowing for an arbitrary packing (rectangular, hexagonal, ...) and conductors of an arbitrary cross-section (round, rectangular, ...) [10]. By way of example, this approach is used for characterising two different conductors and packings, and will allow to homogenize the winding in a 2D axisymmetric model of an inductor. The results obtained are compared to those obtained with a fine FE model in which each turn is modelled and discretized.

Manuscript received June 7, 2004. The research was carried out in the frame of the Inter-University Attraction Pole P5/34 for fundamental research funded by the Belgian federal government.

J. Gyselinck is with the Department of Electrical Engineering, Free University of Brussels, Belgium (johan.gyselinck@ulb.ac.be). P. Dular is with the Institut Montefiore, Department of Electrical Engineering, University of Liège, Belgium; he is a Research Associate with the Belgian National Fund for Scientific Research (F.N.R.S.).

II. Skin and proximity effect

A. Definitions and notations

A sinusoidal regime at frequency f (or pulsation $\omega = 2\pi f$) is assumed throughout this paper. A sinusoidally varying quantity, e.g. a current $I(t) = \sqrt{2} I_e \cos(\omega t + \phi)$, is represented by the complex number (in bold) $\boldsymbol{I} = I_e e^{\boldsymbol{i}\phi}$, where I_e is the r.m.s. or effective value of the current ($I_e = \sqrt{\boldsymbol{I}\boldsymbol{I}^*}$, * denotes conjugate value) and $\boldsymbol{i}$ the imaginary unit ($\boldsymbol{i} = \sqrt{-1}$).

A winding of n periodically spaced identical conductors (*wires*, *turns*) is considered. The conductors have a cross-sectional surface area Ω_c, length l, conductivity σ (or resistivity $\rho = 1/\sigma$) and permeability $\mu = \mu_0$ (or reluctivity $\nu = \nu_0 = 1/\mu_0$). The insulating space between the conductors is nonmagnetic ($\nu = \nu_0$); the fill factor of the winding is denoted by λ.

The n conductors, connected in series, carry the same (net) current $\boldsymbol{I}$. For low frequencies, or for a direct current, the Joule losses P are given by $R_{DC} I_e^2 = R_{DC} |\boldsymbol{I}|^2$, where R_{DC} is the DC resistance, i.e. $\rho l/\Omega_c$ for one conductor and $n\rho l/\Omega_c$ for the complete winding. Due to the time-variation of the current $I(t)$ and the transverse magnetic induction $B(t)$ "seen" by the conductors, the current density $j(x, y, t)$ is non-uniform in their cross-section (in the xy-plane), which leads to higher Joule losses $P = nl \int_{\Omega_c} \rho j_e^2 d\Omega$. Commonly, two effects are distinguished and the associated losses simply added: skin effect ($\boldsymbol{I} \neq 0$, $\boldsymbol{B} = 0$) and proximity effect ($\boldsymbol{I} = 0$, $\boldsymbol{B} \neq 0$).

The analytical expressions for round conductors, given hereafter, will further serve as reference for the more general case. The *equivalent radius* of the conductors, of arbitrary cross-sectional shape, is given by $r = \sqrt{\Omega_c/\pi}$. By dividing this radius by the skin depth $\delta = \sqrt{2/(\sigma\omega\mu_0)}$, we obtain the unitless parameter $X = r/\delta = \sqrt{f} \cdot r\sqrt{\pi\sigma\mu_0}$, which will further be referred to as *reduced frequency* [3].

B. Isolated circular conductor: analytical solution

We consider a single, isolated round conductor of (equivalent) radius r. The increase of Joule losses due to skin effect is a function of the reduced frequency X [9]:

$$p_I(X) = \frac{R_{AC}}{R_{DC}} = \frac{X}{2} \operatorname{Re}\left((1+\boldsymbol{i}) \frac{\boldsymbol{J}_0\big((1+\boldsymbol{i})X\big)}{\boldsymbol{J}_1\big((1+\boldsymbol{i})X\big)} \right), \quad (1)$$

with $\boldsymbol{J}_\alpha$ the Bessel function of the first kind and order α.

The conductor is now placed in a spatially uniform in-

duction $\boldsymbol{B}$. The proximity losses are [9]

$$P_B = p_B(X)\,\frac{\pi}{4}\sigma l r^4 \omega^2 B_e^2\,, \tag{2}$$

where the dimensionless factor p_B is given by

$$p_B(X) = \frac{4}{X^2}\ \mathrm{Im}\left(\frac{\boldsymbol{J}_2\big((1+\boldsymbol{i})X\big)}{\boldsymbol{J}_0\big((1+\boldsymbol{i})X\big)}\right). \tag{3}$$

For sufficiently low frequency ($X \to 0$), p_B tends to 1.

C. Conductors of arbitrary cross-section: FE model

In view of a complete eddy current effect characterization of conductors of arbitrary cross-section, a representative 2D FE model comprising a limited number of elementary cells is used. Each such elementary cell, of cross-sectional area Ω, contains one conductor cross-section and the surrounding insulation (with $\lambda = \Omega_c/\Omega$). The FE model consists of a central cell and n_l surrounding layers of cells, with $n_l \geq 0$. Figs. 1 and 2 show the FE model with $n_l = 1$ for the two different winding types that will be considered in the following: round conductors with hexagonal packing and rectangulars conductors with rectangular packing respectively. The conductor surface area $\Omega_c = 1\,\mathrm{mm}^2$ (or equivalent radius $r = 0.5642\,\mathrm{mm}$) and the fill factor $\lambda = 0.8225$ are the same in both cases. A conductivity $\sigma = 6 \cdot 10^7\,\mathrm{S/m}$ is further assumed.

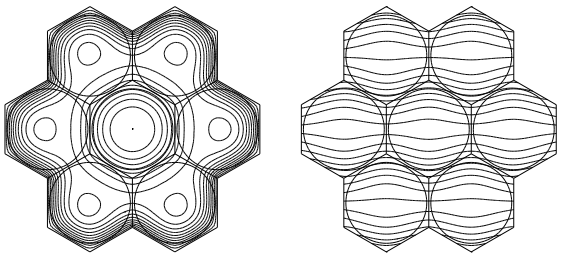

Fig. 1. Round conductors (radius $r = 0.5642\,\mathrm{mm}$) with hexagonal packing – elementary flux pattern for skin effect (left) and proximity effect (right), both for $X = 2$

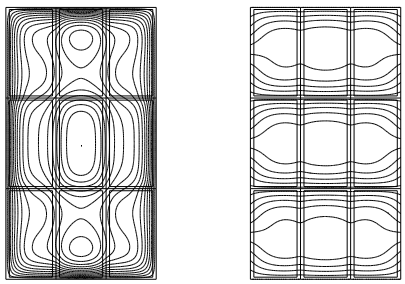

Fig. 2. Rectangular conductors ($1.4142 \times 0.7071\,\mathrm{mm}^2$) with rectangular packing ($1.4827 \times 0.82\,\mathrm{mm}^2$) – elementary flux pattern for skin effect (left) and proximity effect (right), both for $X = 2$

Time-harmonic finite eddy current calculations using the well-known magnetic vector potential (MVP) formulation [11] are carried out. The three (scalar) quantities of interest for the homogenization are the net current $\boldsymbol{I}$ in the conductors and the two components of the average induction in the *central cell*, $\{\boldsymbol{B}_x, \boldsymbol{B}_y\}$. The current $\boldsymbol{I}$ is straightforwardly enforced in each conductor [11]. By means of the following condition on the outer boundary

$$\boldsymbol{a}(x,y) = y\boldsymbol{B}'_x - x\boldsymbol{B}'_y\,, \tag{4}$$

where $\boldsymbol{a}(x,y)$ is the z-component of the MVP, the average induction $\{\boldsymbol{B}'_x, \boldsymbol{B}'_y\}$ in the *complete FE model* can be imposed. In general, this latter induction value differs (slightly) from $\{\boldsymbol{B}_x, \boldsymbol{B}_y\}$. In practice, by exploiting symmetry and/or linearity, a quickly converging iterative scheme can be used to find the excitation $\{\boldsymbol{I}, \boldsymbol{B}'_x, \boldsymbol{B}'_y\}$ producing the wanted values $\{\boldsymbol{I}, \boldsymbol{B}_x, \boldsymbol{B}_y\}$.

With $\{\boldsymbol{I}, \boldsymbol{B}_x, \boldsymbol{B}_y\}$ equal to $\{1,0,0\}$, $\{0,1,0\}$ and $\{0,0,1\}$ respectively, three elementary solutions ($k = 1,2,3$) and the associated current density $\boldsymbol{j}_k(x,y)$ and induction $\{\boldsymbol{b}_x(x,y), \boldsymbol{b}_y(x,y)\}_k$ in the central cell, are readily obtained.

The complex power $\boldsymbol{S}$ absorbed by the central cell, see e.g. [4], given by

$$\boldsymbol{S} \;=\; P + \boldsymbol{i}Q \;=\; l\int_\Omega \left(\rho j_e^2 + \boldsymbol{i}\,\omega\nu_0 b_e^2\right) d\Omega\,, \tag{5}$$

is a quadratic form in $\{\boldsymbol{I}, \boldsymbol{B}_x, \boldsymbol{B}_y\}$, the complex coefficients of which are obtained by integrating the product of the corresponding two elementary solutions over the central cell. With both the real and the imaginary part of $\boldsymbol{S}$, active power P and reactive power Q, can be associated a 3×3 complex Hermitian matrix (transposed matrix equal to conjugate). These two matrices give a complete skin and proximity effect characterization of the winding. In the general case where the conductor does not have any symmetry, the matrices have no other property besides the fact that they are Hermitian. Such a (rather academic) case, viz a round conductor with an eccentric hole, is treated in [10]. The coupling between skin and proximity effect is evidenced.

D. Conductors of symmetric cross-section

In more practical cases, as the ones treated in this paper (Figs. 1 and 2), the conductors are symmetric with respect to x and y axes. Thanks to the spatial orthogonality of the three elementary solutions, there is no coupling between the three excitation modes, and, in particular, skin and proximity effect are uncoupled.

With the complex power absorbed in the central cell due to the current $\boldsymbol{I}$ flowing in the conductors can be associated a complex impedance $\boldsymbol{Z}_{skin}(X)$:

$$\boldsymbol{Z}_{skin} = \frac{\boldsymbol{S}_{skin}}{I_e^2} \;=\; p_I(X)\ R_{DC} + \boldsymbol{i}\ q_I(X)\ \omega\frac{\mu_0 l}{8\pi}\,. \tag{6}$$

The expression for the imaginary part in (6), which is usually negligible (see below), is based on the inductance of a round conductor (internal field only). The unitless factors $p_I(X)$ and $q_I(X)$ follow from the first elementary solution.

Analogously, for an induction $\boldsymbol{B}$ in a certain direction, the complex power $\boldsymbol{S}$ can be written as

$$\frac{\boldsymbol{S}_{prox}}{l\Omega\, B_e^2} \;=\; p_B(X)\ \frac{1}{4}\lambda\sigma r^2\omega^2 + \boldsymbol{i}\ q_B(X)\ \omega\nu_0, \tag{7}$$

where the expression for the real part is based on the analytical expression (2) for low-frequency proximity losses in a round conductor ($\pi R^2 = \lambda\Omega$). The unitless factors $p_B(X)$ and $q_B(X)$ for induction in x and y direction follow from the second and third elementary solution respectively.

Figs. 3 and 4 give the frequency dependence ($0.1 \leq X \leq 3$) of the skin and proximity effect coefficients obtained with the FE models depicted in Figs. 1 and 2 respectively. (Note that for the dimensions chosen, X equal to 0.1, 1, 2 and 3 corresponds to f equal to 132.6 Hz, 13.26 kHz, 53.05 kHz and 119.4 kHz.) These results are obtained with one layer

of cells around the central cell ($n_l = 1$). This is sufficiently accurate for the cases considered: e.g., for the round conductor and $p_B(X = 2)$, $n_l = 0$ gives a 1.4% higher value, and $n_l = 2$ a 0.015% lower value.

The anisotropy of the round conductor with hexagonal packing has been found to be negligible, which is obviously not the case for the rectangular conductor.

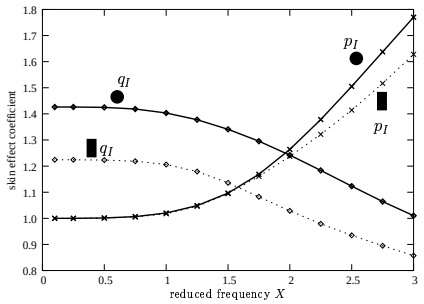

Fig. 3. Skin effect coefficients p_I and q_I versus reduced frequency X for the two conductors

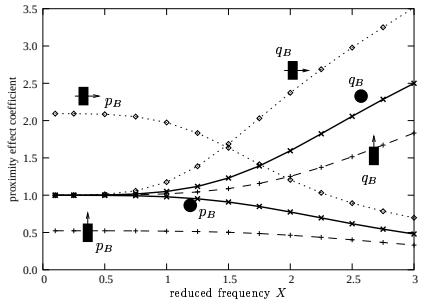

Fig. 4. Proximity effect coefficients p_B and q_B versus reduced frequency X for the two conductors (for the rectangular conductors, flux along either x-axis or y-axis)

Further calculations confirm some observations done in [9], namely that the skin effect losses (coefficient p_I) depend little on the fill factor λ, unlike the proximity losses (coefficients p_B and q_B).

III. Homogenization of winding 2D FE model

In a 2D FE model, with either translational or axial symmetry and either in the time or the frequency domain, the eddy currents in a multi-turn winding can be modelled directly and precisely by defining each conductor as a so-called *massive conductor* [11]. As a rule of thumb, the characteristic length of the discretization of the conductors, denoted by l_c, has to be at least three times smaller than the skin depth δ. This quickly results in a prohibitively large number of unknowns. Furthermore, the additional electrical circuit equations for allowing a voltage supply of the winding or the coupling with an external circuit, have a detrimental effect on the conditioning of the system matrix and thus on the computation time.

In the frequency domain, the eddy current effects can be easily taken into account by means of a homogenization technique [9], [4]. The complete winding is then modelled as a so-called *stranded conductor*, in which a uniform current density $\boldsymbol{j} = n\boldsymbol{I}/\Omega_w$, with n the number of conductors (wires, turns) and $\Omega_w = n\Omega_c/\lambda$ the overall surface area, is adopted [11]. A fine discretization of the winding domain Ω_w, linked to the skin depth, is not required. On the basis of the above complex power considerations (5), the proximity losses can be simply effected by means of a complex and frequency dependent reluctivity tensor $\boldsymbol{\nu}_{prox}$:

$$\boldsymbol{\nu}_{prox} \;=\; q_B(X)\;\nu_0 + \boldsymbol{i}\;p_B(X)\;\frac{1}{4}\lambda\sigma r^2\omega \qquad (8)$$

For round conductors, this tensor can be reduced to a scalar quantity. For rectangular conductors, with the sides parallel to x and y axes, the tensor is diagonal.

Further, in the electrical circuit equation linking the terminal voltage of the winding, $\boldsymbol{U}$, to the current $\boldsymbol{I}$ and the vector potential $\boldsymbol{a}$ [11], the DC resistance R_{DC} has to be replaced by impedance $\boldsymbol{Z}_{skin}$ defined in (6).

IV. Application example

The homogenization method will now be applied to a 2D axisymmetric FE model of an inductor. Its 144-turn winding is made of either of the two conductors characterized in section II (same cross-section and fill factor). The inductor model with round conductors and hexagonal packing is depicted in Fig. 5. In case of rectangular conductors and rectangular packing, the longest side of conductor cross-section is either in radial direction (along x-axis) or vertical (along y-axis), as shown in Fig. 6.

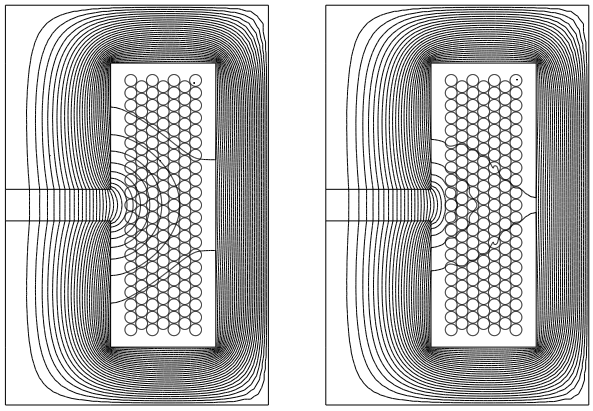

Fig. 5. 2D axisymmetric model of inductor (round conductors and hexagonal packing, total inductor height 38 mm, outer radius 25 mm, height of winding window 27 mm, outer radius 20 mm, airgap thickness 3 mm and radius 10 mm) – flux lines (real part) with imposed unit current $\boldsymbol{I} = 1$, at $X = 0.1$ (left) and $X = 2$ (right)

This results in three different windings (having the same DC resistance of 0.22 Ω), for which time-harmonic calculations with imposed unit current $\boldsymbol{I} = 1$ are carried out, with the reduced frequency X ranging from 0.1 to 2. Both a fine model and a homogenized model are used. In the former model, each of the 144 conductors is finely discretized ($l_c = r/8$), leading to a total of 84000 to 92000 real unknows and a computation time of 200 CPUs (on a Pentium 4, 2 GHz) for one time-harmonic calculation. In the homogenized model, the discretization of the winding cells is much coarser ($l_c = r$),which results in ten times less unknowns, viz 8000 to 9000, and a calculation time of only 1.5 s.

Some flux patterns are shown in Figs. 5 and 6. In the latter figure, one clearly observes the anisotropic eddy current effect.

Figure 7 represents the vertical induction component along a radial line (10 mm $\leq x \leq$ 20 mm, $y = 0$) situated in the horizontal symmetry plane and cutting the winding. The induction obtained with the fine model clearly shows

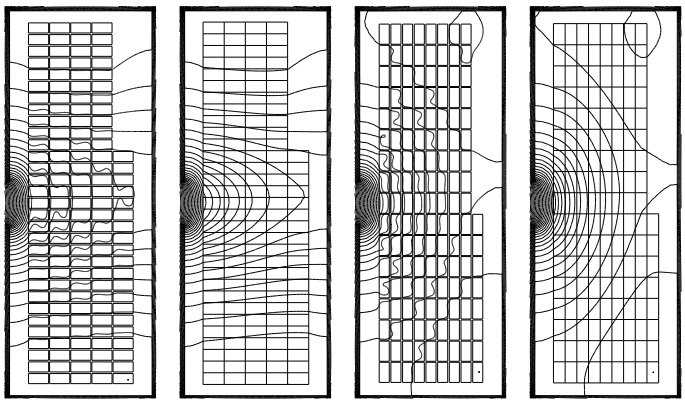

Fig. 6. Winding with rectangular conductors (two orientations) – flux lines (real part, with imposed unit current $\boldsymbol{I} = 1$, $X = 2$) in winding window, obtained with fine and homogenized model

the trace of the individual conductors located on the line or adjacent to it.

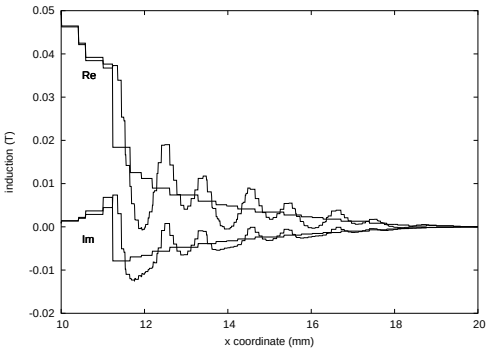

Fig. 7. Vectical induction component (real and imaginary part) versus x-coordinate, with round conductors and $X = 2$, obtained with fine model (thin line) and homogenized model (thick line)

The impedance of the inductor, $\boldsymbol{Z} = \boldsymbol{S}/I^2 = R + \boldsymbol{i}\omega L$, is calculated via the complex power $\boldsymbol{S}$. For the fine model, $\boldsymbol{S}$ is directly evaluated using (5); for the homogenized model, this is done using $\boldsymbol{\nu}_{prox}$ and $\boldsymbol{Z}_{skin}$. Figure 8 shows the resistance R and the inductance L as a function of the reduced frequency X. For all three windings a very good agreement is observed between the impedance obtained with the fine model and with the homogenized model.

Note that with increasing frequency, the contribution of the skin effect losses to the total Joule losses quickly becomes negligible (compare $p_I(X)R_{DC}$ with the total inductor resistance R for e.g. $X = 1$). One also verifies that the contribution of the q_I-term in (6) to the total inductance is negligible: $1\,\mu$H (or less) compared to $3.5\,$mH (or more).

V. Conclusions

For windings with round and rectangular conductors, the homogenization method presented amounts to the usage of a frequency-dependent resistance and a complex frequency-dependent reluctivity tensor. The value of both is obtained using a computationally cheap 2D FE model. The real-life application example clearly demonstrates the ease of implementation, the accuracy and the favorable computation time of the homogenization method. After this numerical validation stage, future work will comprise experimental valdation and extension of the homogenization method to the time domain.

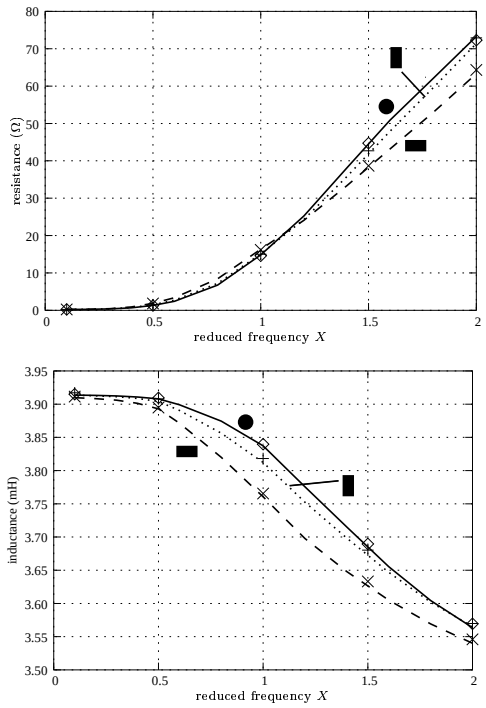

Fig. 8. Resistance (up) and inductance (below) versus reduced frequency X, obtained with fine model (markers $\diamond$, $+$, $\times$) and homogenized model (lines)

References

[1] P. Dowel, "Effects of eddy currents in transformer windings", *Proc. IEEE*, vol. 113, pp. 1387–1394, August 1966.

[2] F. Ferreira, "Improved analytical modeling of conductive losses in magnetic components", *IEEE Trans. Power Electron.*, vol. 9, no. 1, pp. 127–131, January 1994.

[3] F. Robert, P. Mathys and J.-P. Schauwers, "Ohmic losses calculation in SMPS transformers: numerical study of Dowell's approach accuracy", *IEEE Trans. on Magn.*, vol. 34, no. 4, pp. 1255–1257, July 1998.

[4] O. Moreau, L. Popiel and J. L. Pages, "Proximity losses computation with a 2D complex permeability modelling", *IEEE Trans. on Magn.*, vol. 34, no. 5, pp. 3616–3619, September 1998.

[5] C. Larouci, J.-P. Keradec, J.-P. Ferrieux, L. Gerbaud and B. Lebedev, "Copper losses of flyback transformer: search for analytical expressions", *IEEE Trans. on Magn.*, vol. 39, no. 3, pp. 1745–1748, May 2003.

[6] C. Sullivan, "Computationally efficient winding loss calculation with multiple windings, arbitrary waveforms, and two-dimensional or three-dimensional field geometry", *IEEE Trans. on Power Electron.*, vol. 16, no. 1, pp. 142–150, January 2001.

[7] X. Nan and C. Sullivan, "An improved calculation of proximity-effect loss in high-frequency windings of round conductors", in *Proc. IEEE 34th Annual Conference on Power Electronics Specialist (PESC)*, Acapulco, Mexico, June 15–19, 2003, vol. 2, pp. 853–860.

[8] M. Feddi, Z. Ren and A. Razek and A. Bossavit, "Homogenization technique for Maxwell equations in periodic structures", *IEEE Trans. on Magn.*, vol. 33, no. 2, pp. 1382–1385, March 1997.

[9] A. Podoltsev and B. Lebedev, "Analysis of effective resistance and eddy-current losses in multiturn winding of high-frequency magnetic components", *IEEE Trans. on Magn.*, vol. 39, no. 1, pp. 539–548, January 2003.

[10] J. Gyselinck and P. Dular, "Homogenisation of bundles of wires of arbitrary cross-section taking into account skin and proximity effect and their coupling", in *Proc. Fifth IEE International Conferenve on Computation in Electromagnetics (CEM)*, Stratford-upon-Avon, UK, April 19–22, 2004, pp. 137–138.

[11] P. Lombard, G. Meunier, "A general purpose method for electric and magnetic combined problems for 2D, axisymmetric and transient systems", *IEEE Trans. on Magn.*, vol. 29, no. 2, pp. 1737–1740, March 1993.